DCG

GJBX-4(84)

National Uranium Resource Evaluation

CALIBRATION AND PERFORMANCE OF A HIGH-RESOLUTION GAMMA-SPECTROSCOPY SYSTEM

Bendix Field Engineering Corporation
Grand Junction, Colorado

June 1984

PREPARED FOR THE U.S. DEPARTMENT OF ENERGY
Assistant Secretary for Nuclear Energy
Grand Junction Area Office, Colorado

This report is a result of work performed by Bendix Field Engineering Corporation, Operating Contractor for the U.S. Department of Energy, as part of the National Uranium Resource Evaluation. NURE was a program of the U.S. Department of Energy's Grand Junction, Colorado, Office to acquire and compile geologic and other information with which to assess the magnitude and distribution of uranium resources and to determine areas favorable for the occurrence of uranium in the United States.

Available from: Technical Library
Bendix Field Engineering Corporation
P.O. Box 1569
Grand Junction, CO 81502-1569

Telephone: (303) 242-8621, Ext. 278

Price per Microfiche Copy: $4.50

GJBX-4(84)

CALIBRATION AND PERFORMANCE OF A HIGH-RESOLUTION GAMMA-SPECTROSCOPY SYSTEM

Gary Dechant and Stephen Donivan

Bendix Field Engineering Corporation
Grand Junction Operations
Grand Junction, Colorado 81502

June 1984

Prepared for the U.S. Department of Energy
Assistant Secretary for Nuclear Energy
Grand Junction Area Office
Under Contract No. DE-AC07-76GJ01664

CONTENTS

ILLUSTRATIONS

TABLES

EXECUTIVE SUMMARY

One of the primary analytical techniques for the determination of radionuclides is high-resolution gamma-ray spectroscopy. The system used by the Analytical Chemistry Laboratory of Bendix Field Engineering Corporation (Bendix) in support of the U.S. Department of Energy Grand Junction Area Office consists of four Ge(Li) detectors operated under computer control. Quantifying the nuclides of interest is accomplished by comparing the intensities of gamma-ray photopeaks in the samples with those in certified standards after correcting for self-absorption.

The success of this method depends on how well the equipment can be calibrated. This document presents a general description of the calibration techniques used by Bendix for their high-resolution gamma-ray spectroscopy system. Complete descriptions of operating procedures and software documentation are contained in separate manuals.

1.0 INTRODUCTION

A high-resolution gamma-spectroscopy system consisting of four Ge(Li) detectors operated under computer control is used by the Analytical Chemistry Laboratory of Bendix Field Engineering Corporation (Bendix)/Grand Junction Operations for the determination of radium-226, potassium, and equivalent uranium and thorium. Bendix is the operating contractor for the U.S. Department of Energy (DOE) Grand Junction, Colorado, Area Office. Each detector in the system operates independently. Quantifying the nuclides of interest is accomplished by comparing the intensities of gamma-ray photopeaks in the samples with those in certified standards after correcting for self-absorption. The configuration, calibration, and performance of one such detector are described in detail in the sections that follow. The detector described is representative of the entire four-detector system. Detailed operating instructions for this system are provided in a separate procedure manual.

2.0 SYSTEM CONFIGURATION

2.1 GENERAL

The instrumentation and hardware that make up the gamma-spectroscopy system are shown schematically in Figure 1. The sample to be analyzed is positioned on the detector through the access door by the automatic sample changer. Gamma rays in the energy range 50 keV to 3.0 MeV are measured by the detector; the data are stored in the 4096 channels of the Canberra Series 80 Multichannel Analyzer (MCA), and then transferred to the Digital Equipment Corporation (DEC) PDP 11/44 computer at the end of each analysis. The PDP 11/44 stores the data, actuates the sample changer, and resets the MCA for the next analysis. All the equipment is maintained on an Elgar 20-minute uninterruptible power supply.

2.2 DETECTORS

All four detectors are vertically mounted, aluminum-capped, coaxial detectors with factory-matched preamplifiers. The specifications of the individual detectors vary, with efficiencies of 20 to 43 percent and resolutions of 1.5 to 3.8 keV over the energy range analyzed. The resolution and efficiency of each detector are initially checked against certified values, as prescribed by the manufacturer. The top of each detector is fitted with a 1/4-inch plastic protection plate. The detector is then mounted in a low-background shield, constructed by stacking 2-inch-by-4-inch-by-8-inch lead bricks in a pattern that minimizes cracks through the walls. The top and sides of the shield are built to a thickness of 6 inches and the bottom to a thickness of 4 inches. The shield is graded on the inside using 1/4-inch copper sheets to reduce fluoresced lead X-rays. Each shield is constructed on a 1-inch-thick steel plate mounted 3 feet above the floor on concrete pillars. An access hole in the bottom of the shield permits mounting and removal of the detector without shield disassembly. The dewar is mounted below and outside the shield such that the greater part of the detector assembly is inside the shield. A 6-inch-square access hole in the center of the top of the shield permits sample

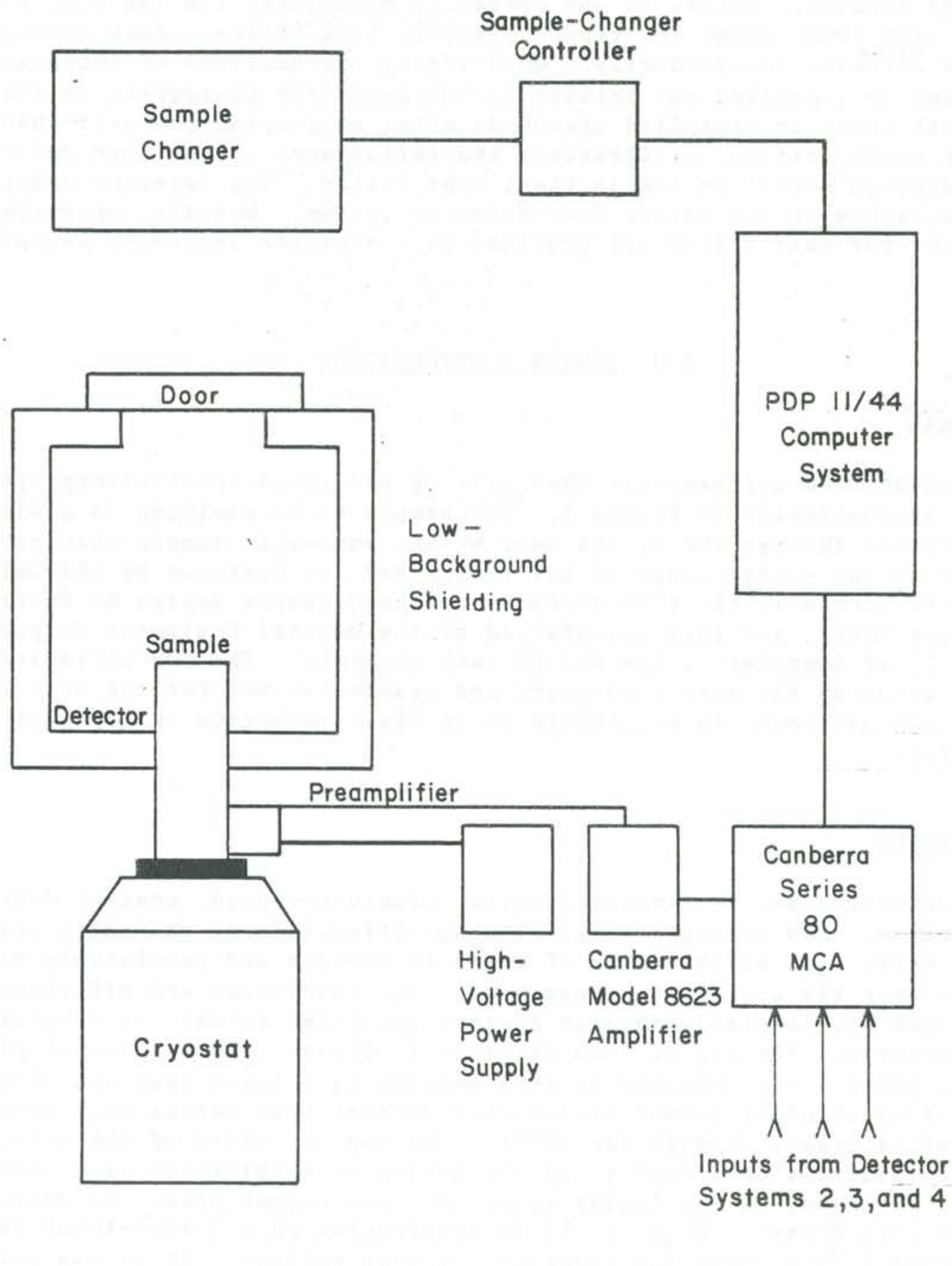

Figure 1. Schematic of Gamma-Spectroscopy System

changing; during analysis, this hole is covered by a 4-inch-thick sliding lead door.

2.3 AMPLIFIERS

Canberra Model 8623 amplifiers are used for all detectors. Functionally, these amplifiers are plug-in signal-processing modules, designed specifically for use with the Canberra Series 80 Multichannel Analyzer. The modules are equipped with pileup rejectors/live-time correctors. For routine operation, the systems are checked for live-time correction and random-summing errors for gross count rates of up to 15,000 counts per second (cps) (see Appendix A). This is equivalent to 1.5 times the gross count rate observed on a 600-gram sample containing 1 percent uranium. Samples exhibiting count rates greater than 15,000 cps are diluted prior to analysis.

2.4 MULTICHANNEL ANALYZER

The amplified signals from the four detectors are routed to a microprocessor-based Canberra Series 80 Multichannel Analyzer (MCA), which interfaces with a DEC PDP 11/44 computer. Such MCA functions as data collection and data transfer are controlled by the computer using FORTRAN-callable subroutines supplied by Canberra. Other MCA functions (peak search, background subtract, etc.) are used only for testing or qualitative analysis. Sample changing, control of analytical conditions, data storage, and data manipulation are performed by the computer for routine quantitative analysis.

2.5 SAMPLE CHANGERS

All detectors are equipped with automatic programmable sample changers, which permit sample analysis on a 24-hour basis. A vacuum suction-cup pickup accommodates a variety of sample containers with only minor adjustments. Consistent sample positioning is maintained by means of adjustable guide rails and rods. The sample changers are interfaced to the PDP 11/44 computer through a Bendix-designed controller that permits operation under program control; the controller monitors sample-changer status during operation to ensure that the proper sample is in place before analysis can proceed.

3.0 DATA COLLECTION AND ANALYSIS

3.1 SAMPLE PREPARATION

Samples to be analyzed are dried at 110°C for 24 hours, then pulverized, blended, and sealed in 441-cc stainless steel cans; a 22-cc can is used if only a small amount of sample is available. Twenty-one days are normally allowed prior to counting to permit radon and its daughters to achieve equilibrium with the radium-226 parent.

3.2 COUNTING PROCEDURE

Samples are counted in batches so sized that each can be completed in a 24-hour period. Sample count times and therefore batch sizes vary, depending on the detection limit and precision desired; typically anywhere from 10 to 25 samples are counted per day. The system is checked on a daily basis by performing a fixed-count-time analysis on a Th-232 standard. Records of peak location, area, and full-width-at-half-maximum for the 238.6-keV Pb-212 peak and the 2614.5-keV Tl-208 peak are maintained for each detector. These data are used to detect problems in sample positioning and to monitor system stability.

Two quality-control samples are included in each sample batch. Statistically repeatable values have been established for these samples, based on a large number of analyses. Records of calculated concentrations, gross count rates, and dead time for each control sample are maintained. Repeat analysis of the entire sample batch is required if the values obtained for either control sample are statistically different from assigned values.

3.3 CALCULATION METHODS

Two FORTRAN programs, GENPEK and GELCAL, are used to perform data analysis and calculations. The function of GENPEK is to store sample number, sample weight, date and time of analysis, and all resolved peaks. Program GELCAL uses the data files generated by GENPEK to calculate nuclide concentrations. These and other related programs are detailed in separate documents.

3.3.1 Determination of Net Peak Area

Program GENPEK first performs a five-point smooth (Savitzky and Golay, 1964) on the raw data, using the equation

$$S_i = [(C_{i-2}+C_{i+2}) + 4(C_{i-1}+C_{i+1}) + 6C_i]/16 \qquad (1)$$

where C_i is the number of observed counts in Channel i and S_i is the number of counts in Channel i in the smoothed spectrum. A smoothed first difference is then calculated from the smoothed raw data to approximate the first derivative of the spectrum, assuming Gaussian-shaped peaks (Adams and Dams, 1970):

$$D_i = [2(S_{i+2}-S_{i-2}) + 1(S_{i+1}-S_{i-1})]/10 \qquad (2)$$

Here, the calculated values for D_i constitute the smoothed first-difference spectrum as shown in Figure 2. Using this smoothed first-difference spectrum, a point-by-point check is made to define the start and end of regions of data containing spectral peaks (Canberra Industries, 1980). The start of a peak region is defined to occur where two consecutive points have a smoothed first difference that exceeds the square root of their original data and where the smoothed first difference of the second point exceeds the smoothed first difference of the first; i.e.,

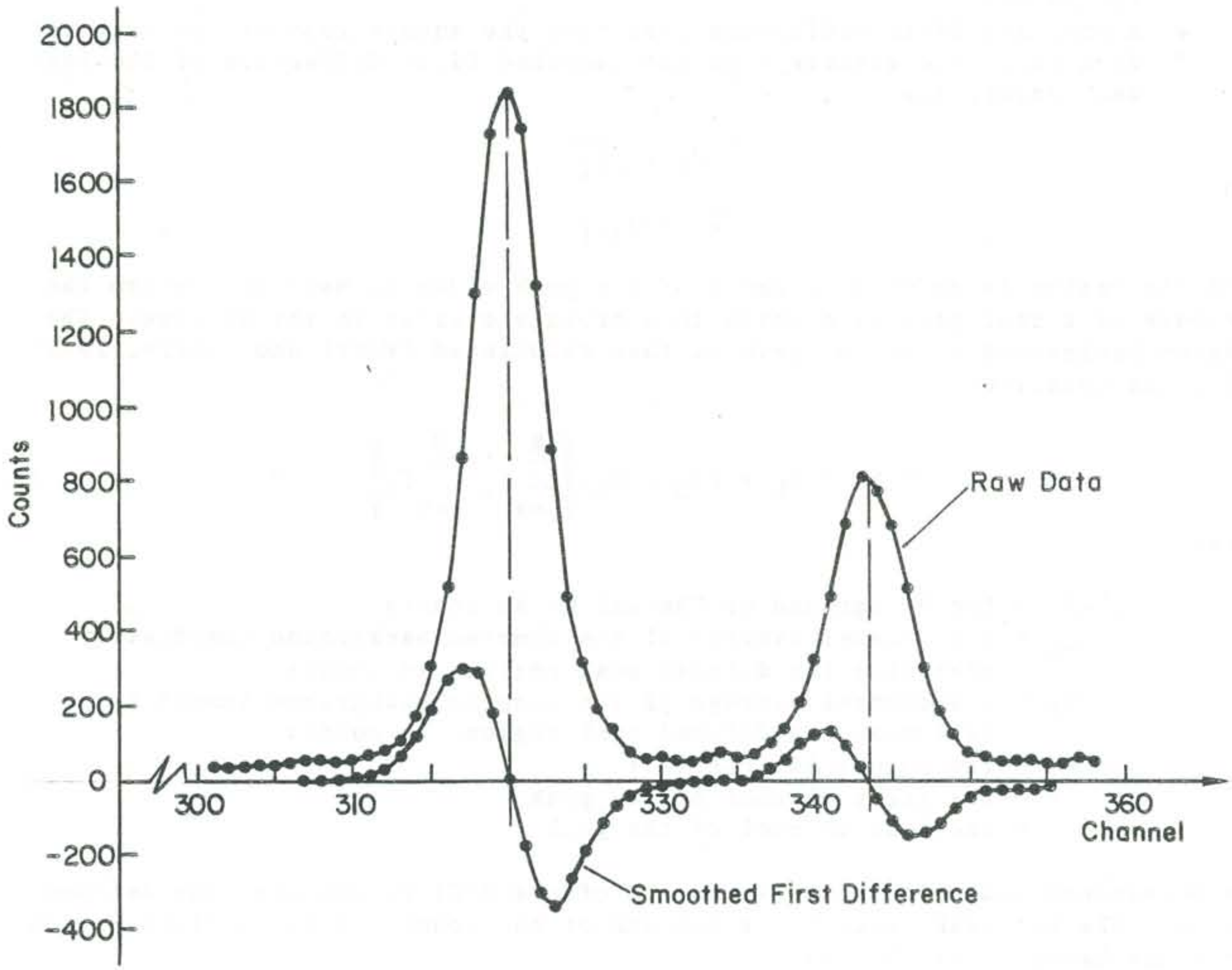

Figure 2. Example of a Smoothed First-Difference Spectrum

$$D_i > \sqrt{C_i}$$

where $C_i > 0$, and

$$D_{i+1} > \sqrt{C_{i+1}}$$

where $C_{i+1} > 0$ and $D_{i+1} > D_i$.

The end of a peak region is defined by one of the following conditions:

- A zero data point ($C_i = 0$).
- A change in the smoothed first difference from negative to positive (or zero).
- A smoothed first difference less than the square root of the original data point and greater than the smoothed first difference of the next data point; i.e.,

$$D_i < \sqrt{C_i}$$

and

$$D_i > D_{i+1}$$

Once the region is defined, a check of the peak width is made to confirm the presence of a real peak as opposed to a broad excursion in the spectra. The Compton background under the peak is then calculated (Murri and others, 1983) using the equation

$$B(K) = B_L + (B_H - B_L)\left[\sum_{i=W}^{K} C_i \quad \sum_{i=W}^{N} C_i\right] \tag{3}$$

where

$B(K)$ = the background at Channel K, in counts
B_L = a 6-channel average of the Compton background immediately preceding the defined peak region, in counts
B_H = a 6-channel average of the Compton background immediately following the defined peak region, in counts
C_i = the counts in Channel i
W = the first channel of the peak
N = the last channel of the peak

The background under the peak is the sum of the B(K) values over the defined region. The net peak area, A, is the sum of the counts in the defined region minus the background; that is,

$$A = \sum_{i=W}^{N} C_i - \sum_{K=W}^{N} B(K) \tag{4}$$

3.3.2 Determination of the Energy of the Peak

The location of the peak is found by searching the smoothed first-difference spectrum for a zero crossing (see Figure 2). The channel assigned as the location is determined by interpolation using the two channels on either side of the zero crossing. This centroid channel is then converted to an energy value using the relationship

$$E = a + zX \tag{5}$$

where

E = energy, in keV
X = channel number
a and z = constants, in keV and in keV per channel

The constants a and z are obtained from a least-squares fit of an energy-versus-channel number plot (see Section 4.1 for further explanation).

3.3.3 Self-Absorption Correction

The net peak area is corrected for self-absorption using the equation

$$R_c = A - [(A)(D_s-D_n)(F_d)] \tag{6}$$

where

R_c = corrected count rate, in cps
A = net peak area, in cps
D_s = sample density, in g/cc
D_n = normalization density (1.36 g/cc)
F_d = correction factor

Refer to Section 4.3 for a detailed discussion of normalization density and determination of the correction factor.

3.3.4 Determination of Nuclide Concentration

Calculations involving detector efficiency are typically used only in the development of correction factors for self-absorption (cf. Section 4.3). However, the following equation is available in the software for special analysis of isotopes for which certified standards are not available (Canberra Industries, 1980):

$$V = R_c/[(Y)(E_f)(w)(0.037)] \tag{7}$$

where

V = nuclide concentration, in pCi/g
R_c = corrected count rate from equation (6)
Y = published branching ratio (Erdtmann and Soyka, 1979)
E_f = detector efficiency [see equation (12) in Section 4.2]
w = sample weight, in grams

Activities can be calculated for isotopes having measurable gamma rays in the range 150 to 3000 keV and known branching ratios.

Program GENPEK calculates the detector efficiency for each peak based on its energy, using the equation

$$\ln E_f = \sum_{i=0}^{n} h_i (\ln E)^i \qquad (8)$$

where

E_f = detector efficiency
E = peak energy, in keV
h_i = constants from efficiency curve (see Section 4.2)
n = 3 or 4 (cf. Section 4.2)

3.3.5 Estimation of the Compton Continuum

The Compton continuum is a function of both the sample matrix and the detector efficiency. An approximation of the Compton continuum as a function of energy is made assuming a reasonably smooth curve following the general detector efficiency function. A series of nonpeak-region data points are used to solve for the l_i values in the general equation

$$C_i = \sum_{i=1}^{4} l_i (\ln E)^i \qquad (9)$$

where

C_i = counts in Channel i
E = energy, in keV
l_i = Compton continuum constants

3.3.6 GAMCAL: Calculation of Nuclide Concentrations

Program GAMCAL calculates concentrations of individual nuclides in the sample using the equation

$$V = [(R_c - B_1)(F_c)]/w \qquad (10)$$

where

V = nuclide concentration, in desired units
R_c = corrected count rate at the analysis energy, in cps
B_1 = system background, in cps (see Section 4.4)
F_c = calibration curve constant (from working curve, Section 4.4)
w = sample weight, in grams

Analysis typically uses the higher energy gamma rays. However, as is the case with uranium and/or thorium, gamma rays of higher intensity but lower energy are also available. If the primary gamma rays are not detected, an additional search of the peak file is performed to determine if a secondary gamma ray was detected (see Section 4.4.1).

If no peak is found, the background count rate, C_i/count time, is calculated from equation (9). A minimum detection limit is calculated using equation (10) where the count rate (R_c-B_1) is determined from the equation

$$(R_c-B_1) = (3.0)(\sqrt{C_B}) + B_1 \tag{11}$$

where

C_B = Compton continuum at the analysis energy, in cps

4.0 CALIBRATION

4.1 ENERGY CALIBRATION

The gamma-spectroscopy system is calibrated for the energy range 50 keV to 3000 keV using the linear function E = a + zX to express the relationship of channel number to energy, where E is energy, X is channel number, and a and z are constants to be determined. Calibration is performed in the following manner.

First, the system is manually set using a Th-232 standard and adjusting the amplifier gain and baseline to place the centroids of the 238.6-keV Pb-212 peak and the 2614.5-keV Tl-208 peak into channels 314 and 3485, respectively. The settings are verified using the peak search function of the MCA.

Once the manual adjustments are in place, spectra of Th-232 and Ra-226 standards are collected and transferred to the computer. Program GENPEK processes the data and outputs channel centroids of the extracted peaks. These centroids along with gamma-ray energies cited in the literature (Erdtmann and Soyka, 1979) are used in a least-squares algorithm to solve for the constants a and z in the equation E = a + zX.

A typical energy-calibration data set is provided in Table 1, together with the magnitude of error in the calibration. Typically, the calibration factor is approximately 0.75 keV per channel, resulting in peak-width-at-half-maximum values of 2 to 5 channels and full-width-at-tenth-maximum values of 8 to 12 channels. The energy calibration plot shown in Figure 3 demonstrates a good fit to the linear function.

Table 1. Typical Energy Calibration Data

Energy of the Peak (keV)	Computed Energy (keV)	Error (percent)
238.63	238.67	0.02
338.40	338.31	-0.03
510.72	510.67	-0.01
583.14	583.55	0.07
860.47	860.75	0.03
911.07	911.08	0.00
968.90	968.87	0.00
2614.47	2614.73	0.01
609.32	609.76	0.07
295.22	294.57	-0.22
1120.28	1119.77	-0.05
1238.11	1238.38	0.02
1764.51	1764.72	0.01
2204.12	2203.53	-0.03

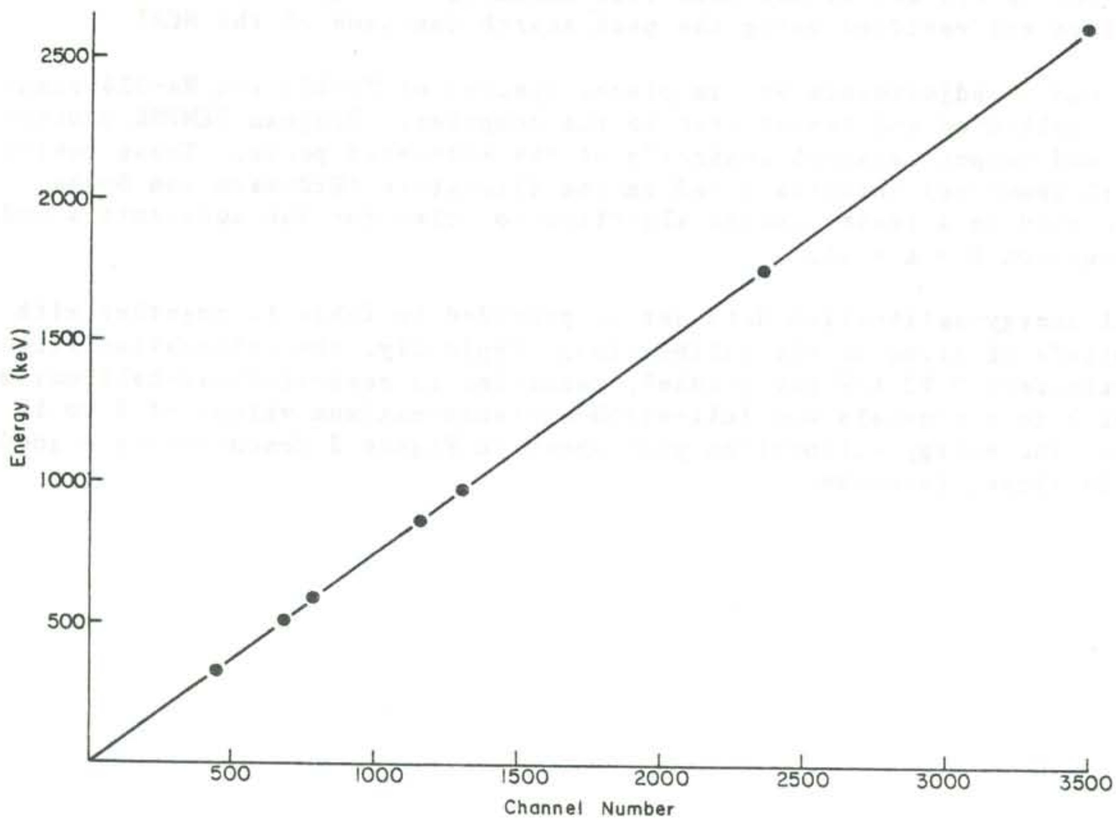

Figure 3. Energy Calibration Plot

4.2 EFFICIENCY CURVE

The typical coaxial Ge(Li) detector demonstrates maximum efficiency in the energy range 150 to 300 keV (Figure 4). For energies from 150 to 3000 keV, the detector efficiency function is best represented by equation (8) (cf. Section 3.3.4):

$$\ln E_f = \sum_{i=0}^{N} h_i (\ln E)^i \tag{8}$$

A fourth-order polynomial is commonly used to fit absolute detector efficiencies since it will approximate the slight dip seen in the efficiency function at 500 to 600 keV and the slight leveling off seen between 1600 and 1800 keV.

Detector efficiencies are experimentally determined using Ra-226 and Th-232 standards (Appendix B) and the peak areas for the gamma rays listed in Table 2. Each efficiency [equation (8)] is based on a fixed sample geometry, and is calculated from the equation

$$E_f = R/(Y \times G \times 37{,}000) \tag{12}$$

where

E_f = efficiency at the energy of the peak
R = measured count rate, in cps
Y = branching ratio (Erdtmann and Soyka, 1979)
G = certified activity of the standard, in microCuries

In the case of small sample sizes, experience has shown that with a fixed geometry and with the sample placed close to the detector, the efficiency function can be approximated with a third-order polynomial. Thus, for routine determinations, n = 3 is used for the 22-cc sample configuration.

Table 2. Gamma-Ray Peaks Used for Efficiency Curve

Ra-226 Isotope	Energy (keV)	Branching Ratio (percent)	Th-232 Isotope	Energy (keV)	Branching Ratio (percent)
Pb-214	295.2	19.20	Pb-212	238.6	43.10
Bi-214	609.3	46.09	Ac-228	338.4	12.01
Bi-214	1120.3	15.04	Tl-208*	510.7	22.50
Bi-214	1238.1	5.92	Tl-208*	583.1	86.0
Bi-214	1764.5	15.92	Ac-228	911.1	29.00
Bi-214	2204.1	4.99	Tl-208*	2614.5	100.00

*Tl-208 branching ratio must be adjusted for 36 percent Tl-208 production (Erdtmann and Soyka, 1979).

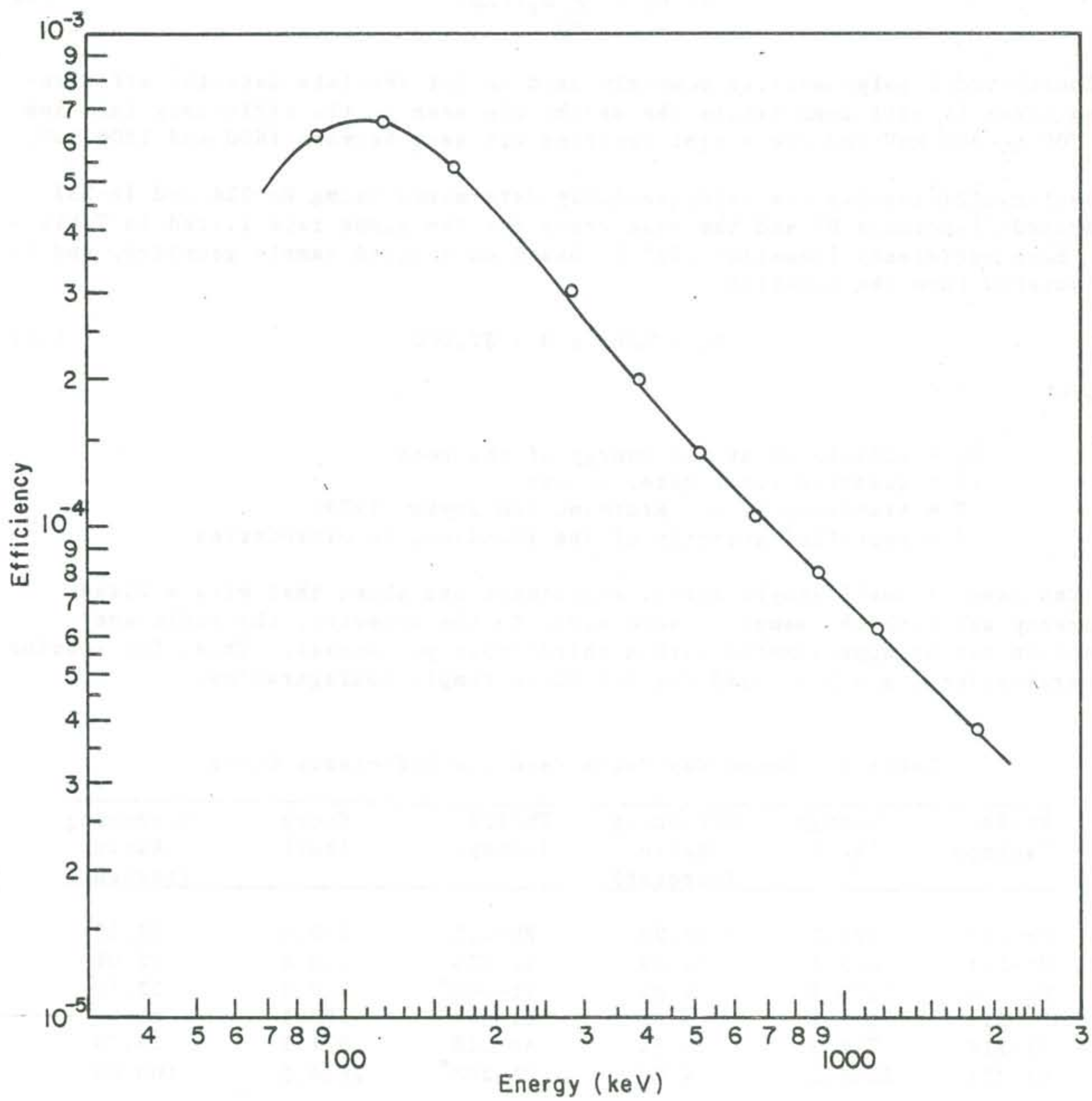

Figure 4. Log-Log Efficiency Plot for a Typical Coaxial Ge(Li) Detector (from Canberra Industries, 1980)

4.3 DENSITY: SELF-ABSORPTION CORRECTION

The attenuation of a gamma ray in a sample of constant volume can be expressed as

$$I = I_o[\mu x/(1 - e^{-\mu x})] \tag{13}$$

where

I = final intensity
I_o = initial intensity
μ = mass attenuation coefficient
x = constant

For the energy range where the Compton effect is the dominant mode of interaction, the mass attenuation coefficient can be approximated using the equation (Adams and Dams, 1970)

$$\mu = \sigma/P = N(Z/A)\sigma \tag{14}$$

where

σ = Compton linear attenuation
P = density, in g/cc
N = Avogadro's number
A = atomic weight
Z = number of electrons

Since Z/A for almost all elements is between 0.4 and 0.5, the mass attenuation coefficient is nearly independent of the nature of the sample. Thus, for the density range in most naturally occurring matrices, the attenuation can be expressed as a linear function of density (Cline, 1977).

A series of Ra-226 and Th-232 standards, with densities ranging from 0.6 to 2.2 g/cc, are prepared (see Appendix B). The samples are analyzed to determine the self-absorption correction function. Efficiency functions for the various densities are calculated (cf. Section 4.2), and the relative variation in efficiency as a linear function of density is determined for a series of energies (Figure 5). All densities are normalized to the density of the efficiency standards (D_n) in order to minimize the required correction. This normalization density approximates the density of samples typically analyzed by the Bendix Analytical Chemistry Laboratory.

The set of energies and their corresponding linear functions (F_d) (Table 3) are fit to the following equation to calculate the d_i constants:

$$F_d = \sum_{i=0}^{3} d_i(\ln E)^i \tag{15}$$

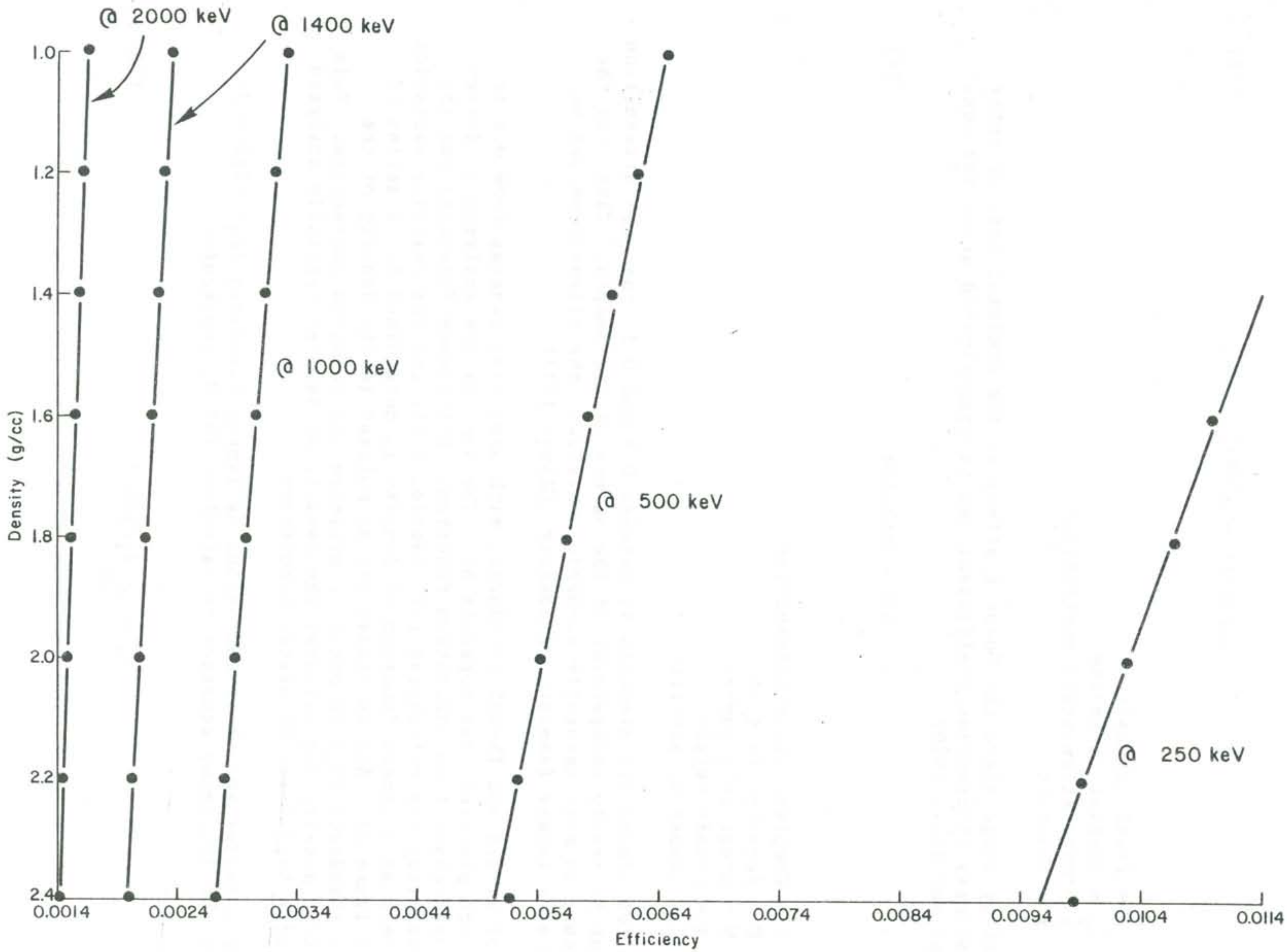

Figure 5. Density Versus Calculated Efficiency for Various Energies

where

F_d = density correction function
d_i = constant
E = energy, in keV

From equation (15), the density correction at any given energy can be calculated. Since the density correction function decreases with an increase in energy, errors in the attenuation correction can be minimized by using higher energy gamma rays.

Table 3. Density Correction Data Set

Energy (keV)	Density Correction Function
185.7	-0.7592
238.6	-0.5464
241.0	-0.5193
295.2	-0.4606
338.4	-0.3399
609.3	-0.2369
1120.3	-0.1662
1238.1	-0.1414
1764.5	-0.1231

4.4 STANDARD CALIBRATION CURVES

Calibration curves are generated using the New Brunswick Laboratory (NBL) 100A Series certified standards for the uranium and thorium decay series (Appendix C). The standards are counted and peak areas determined using GENPEK. From the peak-area values, a linear least-squares curve is fit to the equation

$$V = K(R-B) \tag{16}$$

where

V = nuclide concentration, in desired units
K = constant [see equation (17)]
R = peak count rate, in cps
B = constant environmental background, in cps

The solution to equation (16) is obtained using the relationship

$$K = \Sigma V_i(R_i-B)/\Sigma(R_i-B)^2 \tag{17}$$

where

V_i = individual nuclide concentrations, in desired units
R_i = individual count rates, in cps
B = constant environmental background, in cps

A constant environmental background is shown in Table 4 which presents a typical peak data set for a 3-day empty cave analysis. The primary contribution to this background is attributed to atmospherically borne radon and its daughters, and, at the higher energies, radium within walls, floors, etc. At the large sample size (>300 g), this contribution is reasonably small; however, in the case of small sample sizes (<30 g), special handling for low concentrations is required.

Table 4. Typical Peak Data Set for 3-Day Empty Cave Analysis

Energy (keV)	Net Count Rate (cps)
238	0.01581
296	0.00453
351	0.00834
512	0.02807
558	0.00232
609	0.01026
1120	0.00399
1460	0.04037
1765	0.00395
2614	0.00853

4.4.1 Quantitative Measurements

Calculations based on the working curves described below are considered to be quantitative. These curves are generated using the NBL 100A Series standards 101A-104A and 106A-109A for uranium and thorium, respectively.

4.4.1.1 Equivalent Uranium - Equivalent uranium calibration curve constants are calculated using the peak areas at 1765 keV (primary) and 609 keV (secondary). Both gamma rays are from Bi-214, a Ra-226 daughter. As noted in Section 3.1, use of the Bi-214 daughter requires a preanalysis waiting period of at least 21 days after sealing the can to ensure equilibrium between Bi-214 and Ra-226. In addition, the radium-to-uranium weight ratio for the NBL 100A Series uranium standards is 3.44×10^{-7}, as stated by New Brunswick Laboratory. Since this ratio constitutes a radium/uranium disequilibrium based on an equilibrium ratio of 3.376×10^{-7} (George and Knight, 1982), a disequilibrium correction of 3.44/3.376 is applied to the certified uranium concentrations. Sample concentrations are calculated using the 1765-keV peak count rate whenever this peak is resolved. However, in the case of those low concentrations when the 1765-keV photopeak is not resolved, analysis is performed using the higher intensity 609-keV photopeak. Equivalent uranium concentrations assume radium/uranium equilibrium.

4.4.1.2 Radium-226 - The Ra-226 calibration curves are generated from the same data set as that used for the equivalent uranium curves, except that the NBL-calculated radium values are used for the V_i values in equation (17).

4.4.1.3 Gross Equivalent Uranium - In order to better correlate laboratory analysis with the gross-counting techniques often used in field analysis, a working curve for equivalent uranium based on the sum of the gross counts from 200 to 2900 keV is used. Because the major source of gamma rays in the uranium standards is radium-226 and its daughters, the disequilibrium correction (cf. Section 4.4.1.1) is applied. No density corrections are made in the gross equivalent uranium measurements.

4.4.1.4 Equivalent Thorium - Equivalent thorium measurements use the 2614-keV Tl-208 gamma ray. The lower energy 583-keV Tl-208 gamma ray is used as a secondary peak whenever the 2414-keV gamma ray is not detected.

4.4.1.5 Radium-228 - A Ra-228 calibration curve is generated from the NBL thorium standards, using the 911-keV Ac-228 photopeak. The activities of the standards are calculated by multiplying the micrograms of thorium by 0.1092 (George and Knight, 1982) to convert the certified concentrations to picoCuries of Ra-228.

4.4.1.6 Potassium - A K-40 calibration curve is generated using reagent-grade K_2CO_3 and the 1460-keV gamma ray. Actinium-228, the first daughter of Ra-228, produces a 1459-keV interfering gamma ray. The correction factor for this interference is derived from the ratio of the 911-keV and 1460-keV peak areas in the Th-232 standards. Because of the low count rates associated with K-40, analysis is considered semiquantitative for samples with high Ra-228 concentrations.

4.4.2 Semiquantitative Measurements

The working curves described in this section are based on gamma rays which exhibit low count rates because of low intensity, low efficiency, and/or spectral interference, and are considered semiquantitative.

4.4.2.1 Uranium-238 - Uranium-238 can be measured using the 1001-keV gamma ray from Pa-234m. The NBL uranium standards are assumed to contain the normal isotopic abundance of U-238/U-235. The chemical uranium values are multiplied by 0.993 to correct for the U-235 concentration of the standards. Due to the low intensity of the 1001-keV photopeak, samples with less than 1000 ppm U will not yield a detectable peak using routine counting times.

4.4.2.2 Uranium-235 - Uranium-235 can be measured directly using the 185-keV gamma ray. The U-235 concentrations are calculated by subtracting the U-238 concentration from the total chemical uranium values (cf. Section 4.4.2.1). However, since Ra-226 also exhibits a gamma ray at 185 keV, a correction factor derived from the ratio of the 185-keV and 295-keV peak areas is applied.

5.0 PERFORMANCE

This section contains a general performance evaluation of the gamma-spectroscopy system. Because many of the variables associated with system calibration and routine analysis have uncertainties that are not easily quantified, a series of experimentally measured values were determined to approximate the expected uncertainties. These are categorized as follows:

- Random
  - Counting
  - Weighing
  - Sample Handling
- Working Curve Calibration Constants
- General Evaluation

5.1 RANDOM UNCERTAINTIES

5.1.1 Counting

The relative counting uncertainty is the uncertainty associated with the random nature of the decay process, and is assumed to follow a Poisson statistical distribution for the number of counts in any given channel. The uncertainty in the peak area can then be calculated using the equation

$$\sigma_c = \sqrt{2B + A}/A \tag{18}$$

where

σ_c = relative counting uncertainty
B = Compton background under the peak [equation (3)]
A = net peak area [equation (4)]

5.1.2 Weighing

The uncertainty in the sample weight depends on the balance used. Balances used for weighing the large (441-cc) samples are accurate to ±0.1 g and for the small (22-cc) samples, to ±0.01 g. For samples with densities of 0.5 to 2.0 g/cc, the relative weighing uncertainty will be less than 0.05 percent.

5.1.3 Sample Handling

Sample-handling errors are divided into two general categories, those associated with instrumentation and those associated with sample preparation. The former include equipment fluctuations and sample-detector-positioning fluctuations due to the automatic sample changer. To determine these uncertainties, data from the daily calibration check (cf. Section 3.2) are used. Table 5 presents results of 20 peak-area analyses performed as part of the daily calibration check for each detector system. Since these data represent multiple analysis of a single sample, the weighing and sample preparation errors will not affect the calculated uncertainty. The total uncertainty then represents the uncertainty due to counting and the uncertainty due to instrumentation, etc. The counting uncertainty is calculated using the average counts and equation (18). The total relative uncertainty using the sum-of-squares technique (Bevington, 1969) can be expressed as

$$\sigma_t = \sqrt{\Sigma\sigma_i^2} \tag{19}$$

where

σ_t = total relative uncertainty
σ_i = individual relative uncertainties

Using equation (19), the uncertainty due to instrumentation is solved (Table 5).

Table 5. Repetitive Analyses of the Calibration Sample: Peak Areas in Counts

	System 1	System 2	System 3	System 4
	3630	4466	6903	4369
	3577	4365	7020	4253
	3401	4389	6752	4362
	3489	4134	6858	4343
	3592	4329	6759	4268
	3532	4392	6865	4461
	3646	4215	6959	4494
	3651	4267	6951	4441
	3737	4421	6992	4099
	3552	4293	6885	4260
	3649	4333	6909	4429
	3597	4539	6979	4410
	3607	4326	6860	4404
	3500	4413	6901	4320
	3498	4339	6873	4352
	3467	4368	6895	4405
	3375	4338	7005	4288
	3624	4302	6970	4413
	3538	4255	6609	4318
	3479	4543	6757	4302
Average Counts	3557	4351	6885	4350
Calculated σ	91	99	102	91
Relative σ_t	0.0256	0.0228	0.0149	0.0209
Relative σ, Counting	0.0216	0.0195	0.0131	0.0195
Relative σ, Instrumentation	0.0137	0.0118	0.0071	0.0075

The second category of sample-handling errors, those associated with sample preparation, includes a large number of potential errors; thus, no rigorous evaluation is attempted. In general, errors of this type are considered to be less than 10 percent.

5.2 CALIBRATION CONSTANTS

5.2.1 Density Correction Function

In the case of the large sample cans, the count rate is corrected for attenuation (cf. Section 3.3.3). Determination of this function includes calculations not readily evaluated using normal statistical methods. The count-rate measurements for the calculations are made to within 2 percent relative error. Experience has shown the expected error in this correction factor to be less than 10 percent relative error for energies above 500 keV. Table 6 gives the relative error (in percent) associated with the corrected count rate at various normalized densities, assuming twice the expected error (20 percent) in the correction factor. The relative error cited in Table 6 was calculated using the equation

$$\%\ \text{Error} \cong (D_s - D_n)(F_d)(0.2)(100) \tag{20}$$

where

D_s = sample wt/441 cc
D_n = 1.36
F_d = attenuation correction at the listed energy

and where $(D_s - D_n)F_d \ll 1$. Errors of less than 3 percent can be expected for attenuation correction for routine analysis.

5.2.2 Working Curve Calibration Constant

From equation (17), the uncertainty in the slope, K, is derived (D. C. George, personal communication) using the equation

$$\sigma_K^2 = \left\{ 1/[\Sigma(R_i - B)]^2 \right\} \text{ X } \sum \left\{ [V_i - 2K(R_i - B)]^2 \sigma^2_{(R_i - B)} \right\} \tag{21}$$

The relative uncertainties in K will typically range from 0.5 to 2 percent.

Table 6. Error in Attenuation Correction at Various Normalized Densities

Energy (keV)	Correction Factor	Percent Error 0*	0.68 g/cc*	0.38 g/cc*	0.23 g/cc*
400	0.441	—	6.0	3.2	2.0
500	0.331	—	4.5	2.4	1.5
600	0.254	—	3.5	1.8	1.1
700	0.199	—	2.7	1.4	0.9
800	0.158	—	2.1	1.1	0.7
900	0.128	—	1.7	0.9	0.6
1000	0.105	—	1.4	0.8	0.5
1100	0.089	—	1.2	0.6	0.4
1200	0.076	—	1.0	0.6	0.3
1300	0.067	—	0.9	0.5	0.3
1400	0.061	—	0.8	0.4	0.3
1500	0.054	—	0.8	0.4	0.3
1600	0.055	—	0.7	0.4	0.2
1700	0.055	—	0.7	0.4	0.2
2000	0.055	—	0.7	0.4	0.2

*Absolute value of (D_s-D_n) density.

5.3 GENERAL EVALUATION

The evaluation of errors and uncertainties has, by necessity, involved several assumptions and estimations. To test the validity of these assumptions, a set of 18 duplicates were analyzed for Ra-226 on all four systems using routine sample handling (see Table 7). Data from these analyses were split into two groups (Splits A and B in Table 7), and linear regressions calculated on the two groups.

Table 8 presents results by subsets of the regression analysis of the Ra-226 data given in Table 7. An analysis of Split A versus Split B for each of the four systems (Part I of Table 8) was conducted to evaluate overall sample handling. Results of an analysis of the total sample set on System 1 versus Systems 2, 3, and 4 (Part II of Table 8) were used to evaluate any system biases. Regression lines with a slope of 1.0 and intercepts of 0.0 would be expected if no differences existed between sample sets or between systems.

As the data in Table 8 demonstrate, regression lines for all analyses are approximately 1.0, indicating no significant difference between systems (Part II). Similarly, the intercept values derived from analysis of the total sample set (Part II) indicate no difference between systems.

Table 7. Radium-226 Data from All Four Systems

Sample	Ra-226 (pCi/g)							
	Split A				Split B			
	System 1	System 2	System 3	System 4	System 1	System 2	System 3	System 4
1	55.3	54.8	55.0	53.9	55.7	55.0	56.7	57.1
2	67.5	67.3	67.7	66.4	70.0	68.0	71.0	67.9
3	44.9	45.9	46.8	44.3	46.4	45.4	46.7	46.1
4	34.0	33.7	34.3	33.4	31.9	32.2	32.2	32.6
5	327.4	330.7	324.4	322.8	354.0	355.6	354.3	350.3
6	137.5	137.5	136.9	134.0	148.9	147.3	145.8	147.7
7	680.9	681.5	692.8	684.4	625.0	628.8	631.7	633.8
8	36.0	35.3	35.6	35.6	35.5	35.3	35.3	36.4
9	392.1	391.9	388.8	387.9	397.2	401.4	394.2	401.6
10	128.1	127.5	126.5	128.5	120.4	118.7	123.1	121.9
11	59.0	56.7	56.7	57.5	59.4	58.7	59.5	57.8
12	9.8	9.8	10.0	9.4	11.0	10.7	11.0	11.0
13	17.9	18.5	18.1	18.0	19.1	18.9	19.4	19.5
14	34.3	33.9	33.5	33.7	32.8	32.1	33.0	32.1
15	79.1	79.3	78.3	77.4	75.3	76.8	76.9	77.4
16	315.0	311.3	315.2	314.3	316.1	312.4	318.7	317.0
17	51.8	51.9	52.0	51.8	50.3	50.6	49.2	49.6
18	360.3	364.5	362.8	351.0	366.0	366.9	369.8	363.8

Table 8. Regression Analysis Data

Independent Variable	Dependent Variable	Regression Line	Intercept
I. Comparison of Splits by System*			
A-1	B-1	1.03393	-4.42270
A-2	B-2	1.03049	-3.81304
A-3	B-3	1.03776	-5.49219
A-4	B-4	1.02148	-4.78245
II. Comparison of Systems (all samples)			
System 1	System 2	1.00414	-0.62412
System 1	System 3	1.00387	-0.93965
System 1	System 4	1.00795	-0.77467

*A-1 designates Split A/System 1, etc.

The expected uncertainty for System 1 (excluding counting and sample-preparation uncertainties) can be calculated using equation (19) as follows:

$$\sigma_e = \sqrt{\sigma_1^2 + \sigma_2^2 + \sigma_3^2} \tag{19}$$

$$\sigma_e = 0.017$$

where

σ_e = estimated relative uncertainty
σ_1 = 0.0137 (instrumentation uncertainty from Table 5)
σ_2 = 0.004 [attenuation uncertainty at 1765 keV for $(D_s-D_n)=0.38$]
σ_3 = 0.010 (estimation of working-curve error)

The average relative error for the sample splits analyzed on System 1* can be calculated using values from Table 7 and the equation

$$R_e^2 = \left\{\Sigma[(y_c-b)/b]^2\right\}/(n-1) \tag{22}$$

where

R_e = relative error
y_c = mx + c where x is the value of Split A, m is 1.03393, and c is 4.42270 (from Table 8)
b = value of Split B

The average relative error for this sample set is 0.059. This error is much larger than the expected value of 0.017 calculated above. Since the counting uncertainties are small, it is apparent that the uncertainties due to sample preparation are significantly larger than those due to the analysis. Because sample preparation for this set of samples may or may not be comparable to the other sets, these results can only indicate an approximate order of the uncertainty associated with sample preparation.

---

*Samples with less than 50 pCi/g have significant counting uncertainties and were excluded from this determination.

6.0 REFERENCES

Adams, F., and Dams, R., 1970, Applied gamma-ray spectrometry: Pergamon Press.

Bevington, P. R., 1969, Data reduction and error analysis for the physical sciences: New York, McGraw-Hill.

Canberra Industries, Inc., 1980, Technical reference manual for SPECTRAN-F, Version 1.

Cline, J., 1977, Development of new and improved data reduction techniques for radiometric assay of bulk uranium ore samples: Rockville, Maryland, Science Applications, Inc., Bendix Subcontract No. 77-039-4.

Cline, J., 1982, Bendix (BFEC) PGT Ge(Li) detection efficiency determinations: Rockville, Maryland, Science Applications, Inc.

Currie, L. A., 1968, Limits for qualitative detection and quantitative determination: Analytical Chemistry, v. 40, no. 3, pp. 586-593.

Dickson, B., Christiansen, E., Løvberg, L., and Grasty, R., 1982, Reference materials for calibration of laboratory gamma-ray analyses: Paper submitted to NEA Symposium on Uranium Exploration Techniques.

Erdtmann, G., and Soyka, W., 1979, The gamma rays of the radionuclides: New York, Verlag Chemie.

George, D. C., and Knight, L., 1982, Field calibration facilities for environmental measurement of radium, thorium, and potassium: Grand Junction, Colorado, U.S. Department of Energy, Technical Measurements Center Report GJ/TMC-01(82).

Murri, R., Novak, E., and Ruzycki, C., 1983, Mobile gamma spectroscopy system operation: Grand Junction, Colorado, Bendix Field Engineering Corporation Internal Report No. BFEC-1983-1.

Savitzky, A., and Golay, M., 1964, Smoothing and differentiation of data by simplified least squares procedures: Analytical Chemistry, v. 36, no. 8, pp. 1627-1639.

Appendix A

VERIFICATION OF LIVE-TIME CORRECTION

Performance of the pileup-rejector/live-time-corrector feature on the Canberra Model 8623 amplifiers is verified in the following manner:

1. A cobalt-60 source is mounted above the detector and a spectrum collected.

2. Peak areas and 1- and 2-sigma counting errors are determined.

3. A barium-133 source is mounted near the detector to increase the total gross count rate (channels 3 to 4096) by 1000 counts. The Co-60 peak areas and counting errors are again determined together with the total gross count rate.

4. The Ba-133 source is moved progressively closer to the detector to obtain increases of 500 to 1000 cps in the total gross count rate. At each increment, the Co-60 and total-gross-count-rate data are recorded (Table A-1).

The data in Table A-1 are then plotted (see Figure A-1) to show Co-60 peak areas versus total gross count rate. The 1-sigma error bars for the first count (no Ba-133) are used as upper and lower limits on the graph; all other points are given as ranges set at the 1-sigma counting error.

As Figure A-1 illustrates, for total gross count rates up to 12,000 cps, count rates at the 1-sigma level for all points fall within the upper and lower limits established by the Co-60 source counted alone; thus, live-time correction is considered adequate for the established range. At present, no software corrections for dead time, pileup, or random summing are in place. Instead, amplifiers not meeting the above criterion are replaced or used only for low-level work.

Table A-1. Pileup Rejector Evaluation

Total Gross Count Rate (cps)	Cobalt-60 Area Count Rate (cps) At 1173 keV	Cobalt-60 Area Count Rate (cps) At 1333 keV
3442	206.2 ± 1.0	182.1 ± 0.9
4018	206.3 ± 1.0	180.6 ± 0.9
4758	207.1 ± 1.0	182.4 ± 0.9
5574	206.4 ± 1.0	180.6 ± 0.9
6881	204.5 ± 1.0	180.2 ± 0.9
7934	207.0 ± 1.0	183.1 ± 0.9
8857	204.3 ± 1.0	183.2 ± 0.9
12337	205.8 ± 1.0	184.2 ± 0.9

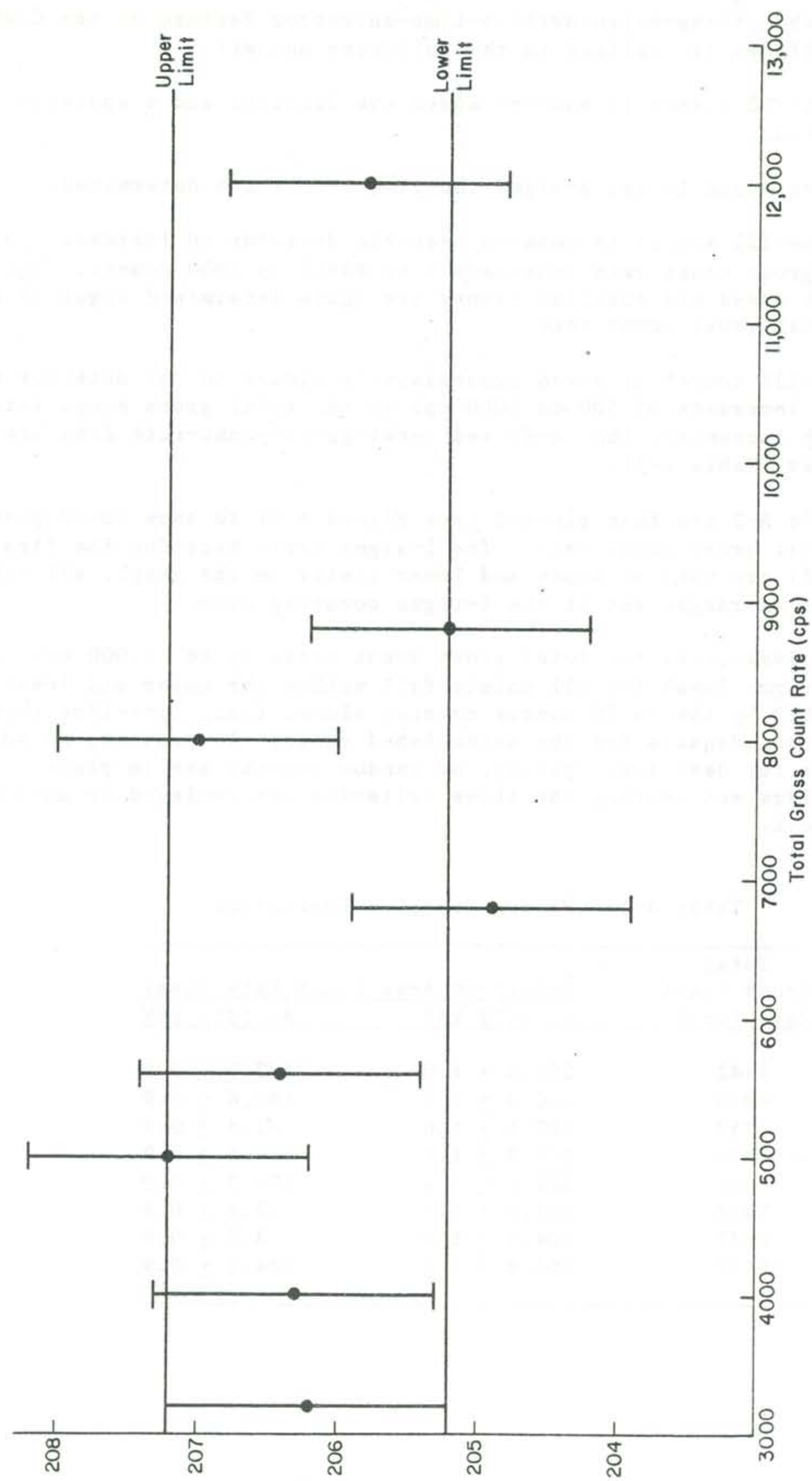

Figure A-1. Pileup Rejector Plot

Appendix B

STANDARD PREPARATIONS

STANDARD SOLUTIONS

RADIUM

The standard radium solution is prepared by diluting a known weight of National Bureau of Standards (NBS) SRM-4959 gamma-ray standard radium-226 solution to 1000 grams with a solution containing 2.0 grams $BaCl_2$ and 120.8 grams HCl per liter.

THORIUM

The standard thorium solution is prepared by dissolving a weighed amount of 50-year-old reagent-grade $Th(NO_3)_4 \cdot 4H_2O$ in 50 to 100 ml of 1N HNO_3 and diluting to 1 liter.

COUNTING STANDARDS

PREPARATION 1

This standard is used as the base for the low-density standards. A weighed portion of the standard solution is added to a calculated volume of 1:1 HNO_3 solution and mixed. An equal volume of tetra-ethyl orthosilicate is then added to the HNO_3 solution and stirred until the solution jells. The jell is heated in a water bath, with stirring, until HNO_3 fumes stop evolving. Heating is continued until the jell has solidified; it is then dried at 110°C overnight. The solid is transferred to a porcelain dish and calcined at 850°C for 1 hour. The calcined sample is weighed and the amount of the standard in picoCuries per gram is calculated. The fused sample is ground by hand to -100 mesh, mixed in a V blender, then packed in the container under 1-ton pressure and sealed hot.

PREPARATION 2

A weighed portion of the standard solution is added to a weighed amount of -100 mesh Ottawa Sand. The mixture is stirred and dried overnight at 110°C. The dried mixture is pulverized by hand, mixed in a V blender, packed under 1-ton pressure, and sealed hot. Adjustments in densities were made by addition of tungsten oxide and/or lead oxide to produce a set of standards with densities ranging from 0.5 to 3.0 g/cc.

Experience has shown that, in rock and soil samples, Ra-226 tends to be segregated into the smaller particle sizes. Because of the frequent use of the NBL calibration standards, settling can occur and result in high values. Thus, all standards are packed under 1-ton pressure and sealed hot to minimize the potential for settling. Standards packed in this manner may be used for up to 100 analyses before reblending is necessary.

Appendix C

URANIUM AND THORIUM DECAY SERIES

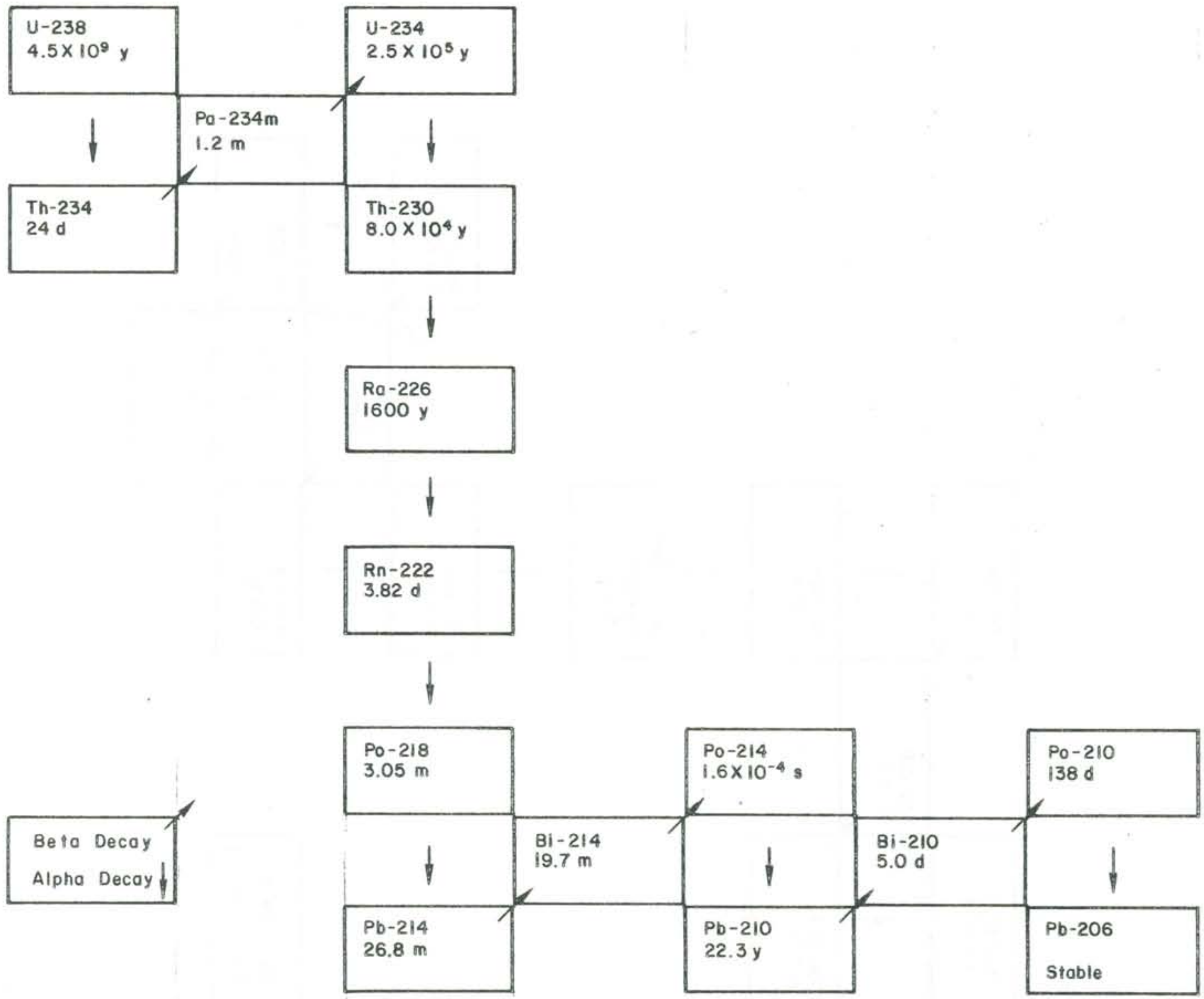

Figure C-1. Principal Decay Scheme of the Uranium Series

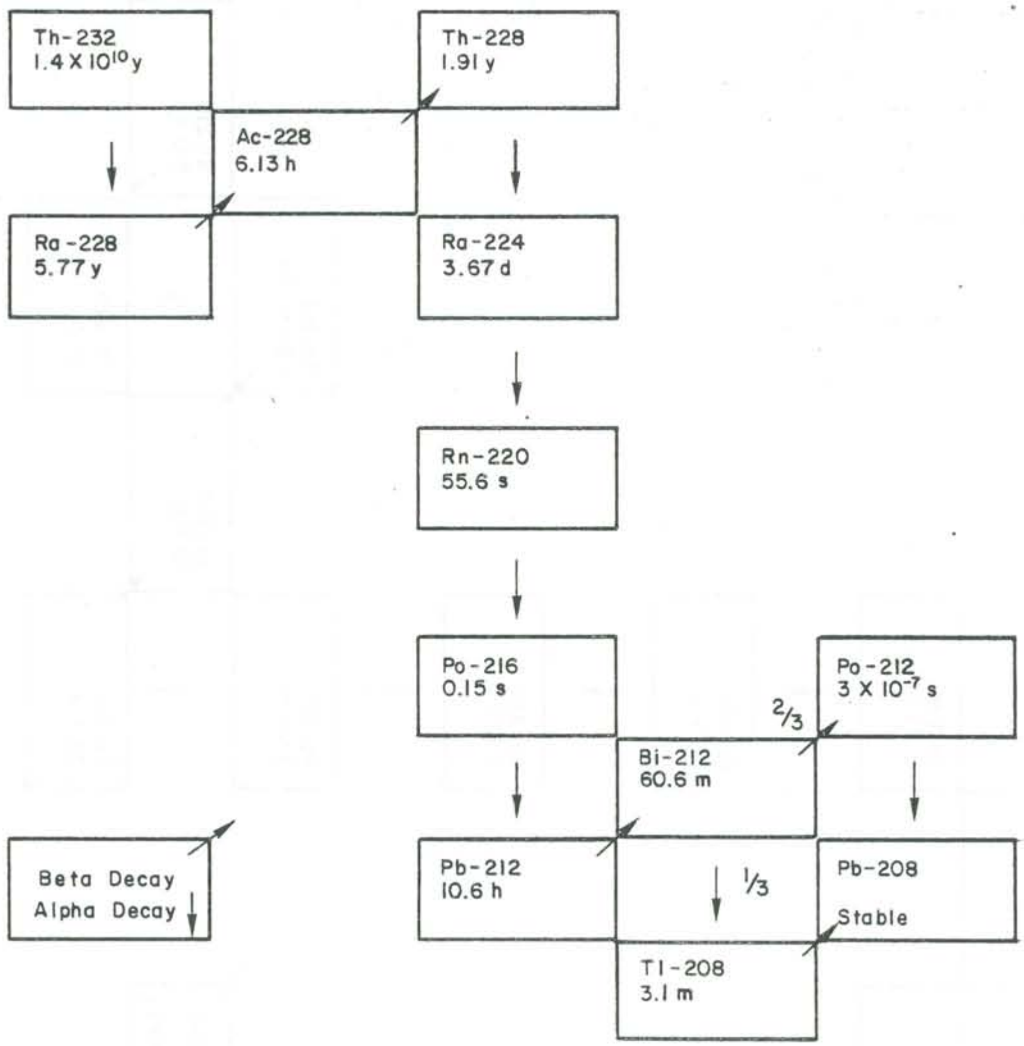

Figure C-2. Principal Decay Scheme of the Thorium Series

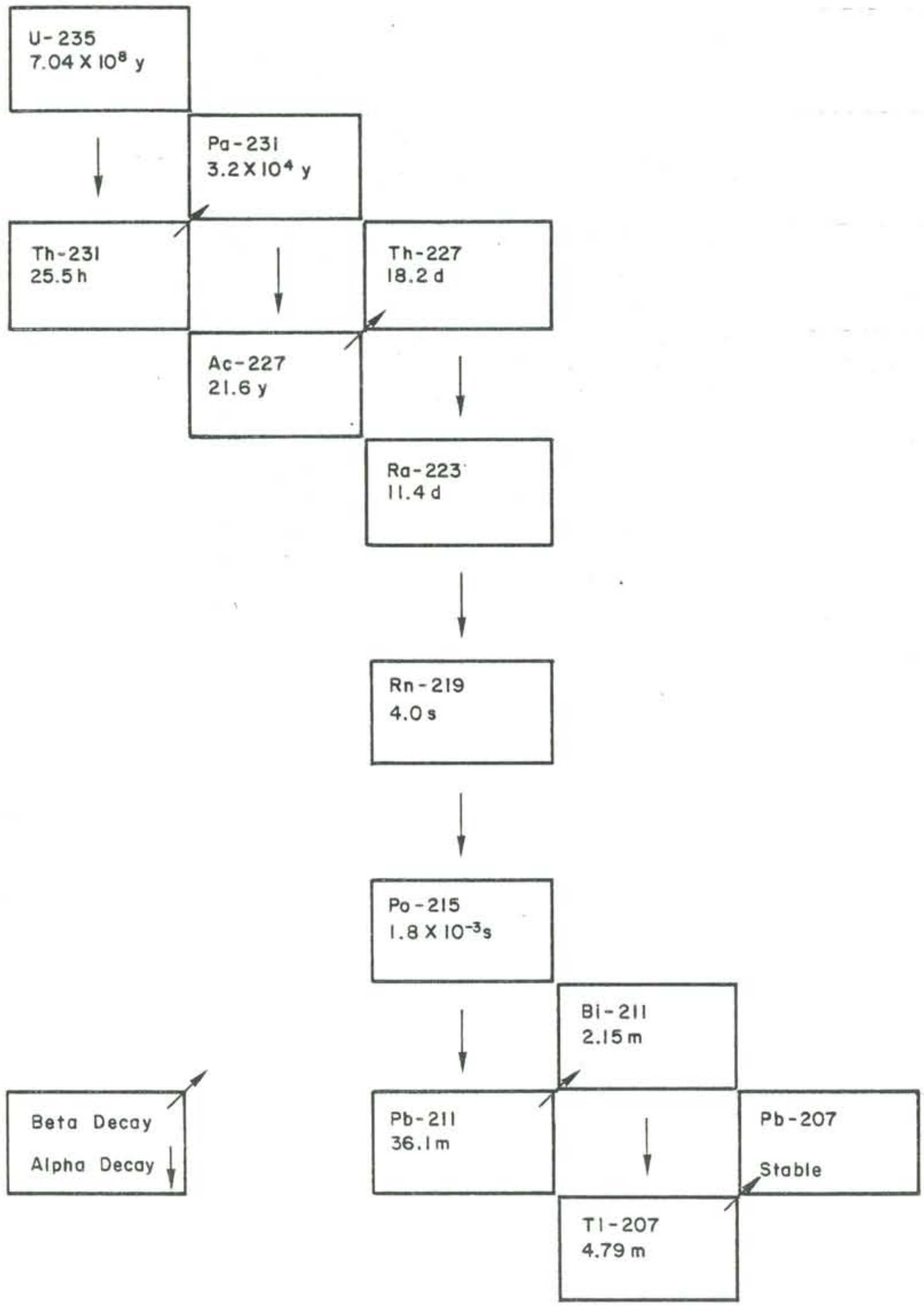

Figure C-3. Principal Decay Scheme of the Actinium Series